



# DIGITAL ACCESS TO SCHOLARSHIP AT HARVARD

## Conversion of Mature Human $\beta$ -Cells Into Glucagon-Producing $\beta$ -Cells

The Harvard community has made this article openly available.  
[Please share](#) how this access benefits you. Your story matters.

<b>Citation</b>	Spijker, H. S., R. B. Ravelli, A. M. Mommaas-Kienhuis, A. A. van Apeldoorn, M. A. Engelse, A. Zaldumbide, S. Bonner-Weir, et al. 2013. "Conversion of Mature Human $\beta$ -Cells Into Glucagon-Producing $\beta$ -Cells." <i>Diabetes</i> 62 (7): 2471-2480. doi:10.2337/db12-1001. <a href="http://dx.doi.org/10.2337/db12-1001">http://dx.doi.org/10.2337/db12-1001</a> .
<b>Published Version</b>	<a href="https://doi.org/10.2337/db12-1001">doi:10.2337/db12-1001</a>
<b>Accessed</b>	February 16, 2015 4:40:05 PM EST
<b>Citable Link</b>	<a href="http://nrs.harvard.edu/urn-3:HUL.InstRepos:12717578">http://nrs.harvard.edu/urn-3:HUL.InstRepos:12717578</a>
<b>Terms of Use</b>	This article was downloaded from Harvard University's DASH repository, and is made available under the terms and conditions applicable to Other Posted Material, as set forth at <a href="http://nrs.harvard.edu/urn-3:HUL.InstRepos:dash.current.terms-of-use#LAA">http://nrs.harvard.edu/urn-3:HUL.InstRepos:dash.current.terms-of-use#LAA</a>

*(Article begins on next page)*

# Conversion of Mature Human $\beta$ -Cells Into Glucagon-Producing $\alpha$ -Cells

H. Siebe Spijker,<sup>1</sup> Raimond B.G. Ravelli,<sup>2</sup> A. Mieke Mommaas-Kienhuis,<sup>2</sup> Aart A. van Apeldoorn,<sup>3</sup> Marten A. Engelse,<sup>1</sup> Arnaud Zaldumbide,<sup>2</sup> Susan Bonner-Weir,<sup>4</sup> Ton J. Rabelink,<sup>1</sup> Rob C. Hoeben,<sup>2</sup> Hans Clevers,<sup>5</sup> Christine L. Mummery,<sup>6</sup> Françoise Carlotti,<sup>1</sup> and Eelco J.P. de Koning<sup>1,5,7</sup>

Conversion of one terminally differentiated cell type into another (or transdifferentiation) usually requires the forced expression of key transcription factors. We examined the plasticity of human insulin-producing  $\beta$ -cells in a model of islet cell aggregate formation. Here, we show that primary human  $\beta$ -cells can undergo a conversion into glucagon-producing  $\alpha$ -cells without introduction of any genetic modification. The process occurs within days as revealed by lentivirus-mediated  $\beta$ -cell lineage tracing. Converted cells are indistinguishable from native  $\alpha$ -cells based on ultrastructural morphology and maintain their  $\alpha$ -cell phenotype after transplantation in vivo. Transition of  $\beta$ -cells into  $\alpha$ -cells occurs after  $\beta$ -cell degranulation and is characterized by the presence of  $\beta$ -cell-specific transcription factors Pdx1 and Nkx6.1 in glucagon<sup>+</sup> cells. Finally, we show that lentivirus-mediated knock-down of Arx, a determinant of the  $\alpha$ -cell lineage, inhibits the conversion. Our findings reveal an unknown plasticity of human adult endocrine cells that can be modulated. This endocrine cell plasticity could have implications for islet development, (patho) physiology, and regeneration. *Diabetes* 62:2471–2480, 2013

**T**he composition and architecture of human islets of Langerhans has been studied for years within their native environment, the pancreas. More recently, the development of islet transplantation as a novel therapeutic option for patients with severe  $\beta$ -cell loss has promoted the study of isolated human islets and single endocrine cells (1). The majority of pancreatic islets consist of two main cell types that together play a key role in glucose homeostasis: insulin-producing  $\beta$ -cells (50–70%) and glucagon-producing  $\alpha$ -cells (20–30%) (1,2). Human islets display a unique architecture that favors contacts between  $\beta$ -cells and  $\alpha$ -cells, while both cell types remain in close relation to the vasculature (3).

$\alpha$ - and  $\beta$ -Cells originate from a common neurogenin 3 (Ngn3)-expressing endocrine progenitor (4). The balance between transcription factors Aristaless-related homeobox (Arx) and paired box4 (Pax4) likely determines the early

fate restriction of  $\alpha$ - and  $\beta$ -cells, respectively (5). Further maturation of  $\beta$ -cells is enabled by the expression of Nkx6.1 (6), while  $\beta$ -cell function is maintained in the adult pancreas by key transcription factors like Pdx1, MafA, and FoxO1 (7).

Strategies to convert postnatal cells derived from the endodermal lineage into endocrine cells have gained much attention in recent years. Forced expression of key transcription factors in murine liver (8,9) or pancreatic cells (10–12) induces conversion into cells with a  $\beta$ -cell phenotype. Furthermore, in mice, near-total loss of  $\beta$ -cell mass causes a small proportion of remaining  $\alpha$ -cells to regenerate  $\beta$ -cell mass (13).

It is generally thought that human endocrine cells do not switch their hormone production once fully differentiated. Without using genetic modification of human islet cells, we now show that  $\beta$ -cells spontaneously convert into glucagon-producing  $\alpha$ -cells during islet cell reaggregation.

## RESEARCH DESIGN AND METHODS

**Human islet isolation and cell culture.** Human islet isolations were performed in the Good Manufacturing Practice facility of our institute according to the method described by Ricordi et al. (14). Islets were dispersed into single cells by adding 0.025% trypsin solution containing 10  $\mu$ g/mL DNase (Pulmozyme, Genentech) at 37°C while pipetting up and down for 6–7 min. The islet cell suspension was plated onto 3% agarose microwell chips containing 2,865 microwells/chip with a diameter of 200  $\mu$ m/microwell (15). Suspension of  $3 \times 10^6$  cells per chip resulted in spontaneous reaggregation of ~1,000 islet cells/microwell. Islet cell aggregates and intact human islets (control) were cultured in CMRL 1066 medium (5.5 mmol/L glucose) containing 10% FCS, 20  $\mu$ g/mL ciprofloxacin, 50  $\mu$ g/mL gentamycin, 2 mmol/L L-glutamin, 0.25  $\mu$ g/mL fungizone, 10 mmol/L HEPES, and 1.2 mg/mL nicotinamide.

**Lentivirus vectors.** pTrip-RIP405Cre-ERT2- $\Delta$ U3 (RIP-CreERT2) and pTrip-loxP-NEO-STOP-loxP-eGFP- $\Delta$ U3 (CMVstopGFP) were kindly provided by P. Ravassard (16). pTrip vectors were produced as third-generation lentivirus vectors by adding a Tat-expressing vector to the regular helper plasmids. The short hairpin (sh)RNA construct against Arx (shArx) was obtained from the MISSION library (clone no. 6591, nontarget control no. SHC-002; Sigma-Aldrich) and produced as previously described (17). For lineage tracing, transduction was performed as previously described (16). Briefly, dispersed islet cells were transduced overnight with a 1:1 mixture of the two lentiviruses at a multiplicity of infection of 2 in regular CMRL medium containing 8  $\mu$ g/mL polybrene. In experiments using the shArx construct, a second round of transduction was subsequently performed for 8 h. 4-hydroxy-tamoxifen (Sigma-Aldrich, St. Louis, MO) was added to a final concentration of 1  $\mu$ mol/L in the evening. After overnight incubation, the medium was refreshed and cells were seeded on the microwell. The start of reaggregation represents day 0 in our experiments.

**RNA isolation and quantitative PCR.** Total RNA was extracted using RNeasy kit (Qiagen) according to the manufacturer's protocol. Total RNA (1  $\mu$ g) was reverse transcribed using M-MLV reverse transcriptase (Invitrogen). Quantitative PCR was performed on a Light Cycler 480-II Real-time PCR system (Roche). Fold induction was calculated using  $\Delta\Delta C_T$  method with human  $\beta$ -actin as housekeeping gene. Primers used are listed in Supplementary Table 1.

**Immunofluorescence staining.** Formalin-fixed islet cell aggregates were washed in PBS and spun down at high speed in fluid agar. Agar-containing cell pellets were embedded in paraffin. Blocks were cut into 4- $\mu$ m sections. Primary

From the <sup>1</sup>Department of Nephrology, Leiden University Medical Center, Leiden, the Netherlands; the <sup>2</sup>Department of Molecular Cell Biology, Leiden University Medical Center, Leiden, the Netherlands; <sup>3</sup>Twente University, Enschede, the Netherlands; the <sup>4</sup>Section of Islet Cell & Regenerative Biology, Joslin Diabetes Center, Harvard Medical School, Boston, Massachusetts; the <sup>5</sup>Hubrecht Institute, Utrecht, the Netherlands; the <sup>6</sup>Department of Anatomy & Embryology, Leiden University Medical Center, Leiden, the Netherlands; and the <sup>7</sup>Department of Endocrinology, Leiden University Medical Center, Leiden, the Netherlands.

Corresponding author: Eelco J.P. de Koning, e.dekoning@lumc.nl.

Received 25 July 2012 and accepted 13 March 2013.

DOI: 10.2337/db12-1001

This article contains Supplementary Data online at <http://diabetes.diabetesjournals.org/lookup/suppl/doi:10.2337/db12-1001/-/DC1>.

© 2013 by the American Diabetes Association. Readers may use this article as long as the work is properly cited, the use is educational and not for profit, and the work is not altered. See <http://creativecommons.org/licenses/by-nc-nd/3.0/> for details.

antibodies against insulin (1:200; Linco), C-peptide (1:1,000; Millipore), glucagon (1:200; Vector and Invitrogen), Pdx1 (1:5; R&D Systems), Nkx6.1 (clone F55A12, 1:1,000; Developmental Studies Hybridoma Bank), Ki67 (1:200; BD Pharmingen), and green fluorescent protein (GFP) (1:500; Roche and Molecular Probes) were used. DAPI (Vector) was used as nuclear counterstaining. Secondary antibodies were TRITC-anti-guinea pig (1:400; Jackson) and Alexa Fluor 488, 568, and 647 anti-mouse or anti-rabbit when appropriate (1:1,000).

Apoptosis was assessed by TUNEL assay (Roche). Sections were examined using confocal microscopy. Staining was quantified as percentage of positive cells per total cell number, counting at least 750 cells per donor for each condition.

**Glucose-stimulated insulin secretion.** Four groups of 30 aggregates per condition were incubated in a modified Krebs-Ringer bicarbonate buffer. Islets were successively incubated for 1 h in Krebs-Ringer bicarbonate buffer with 2

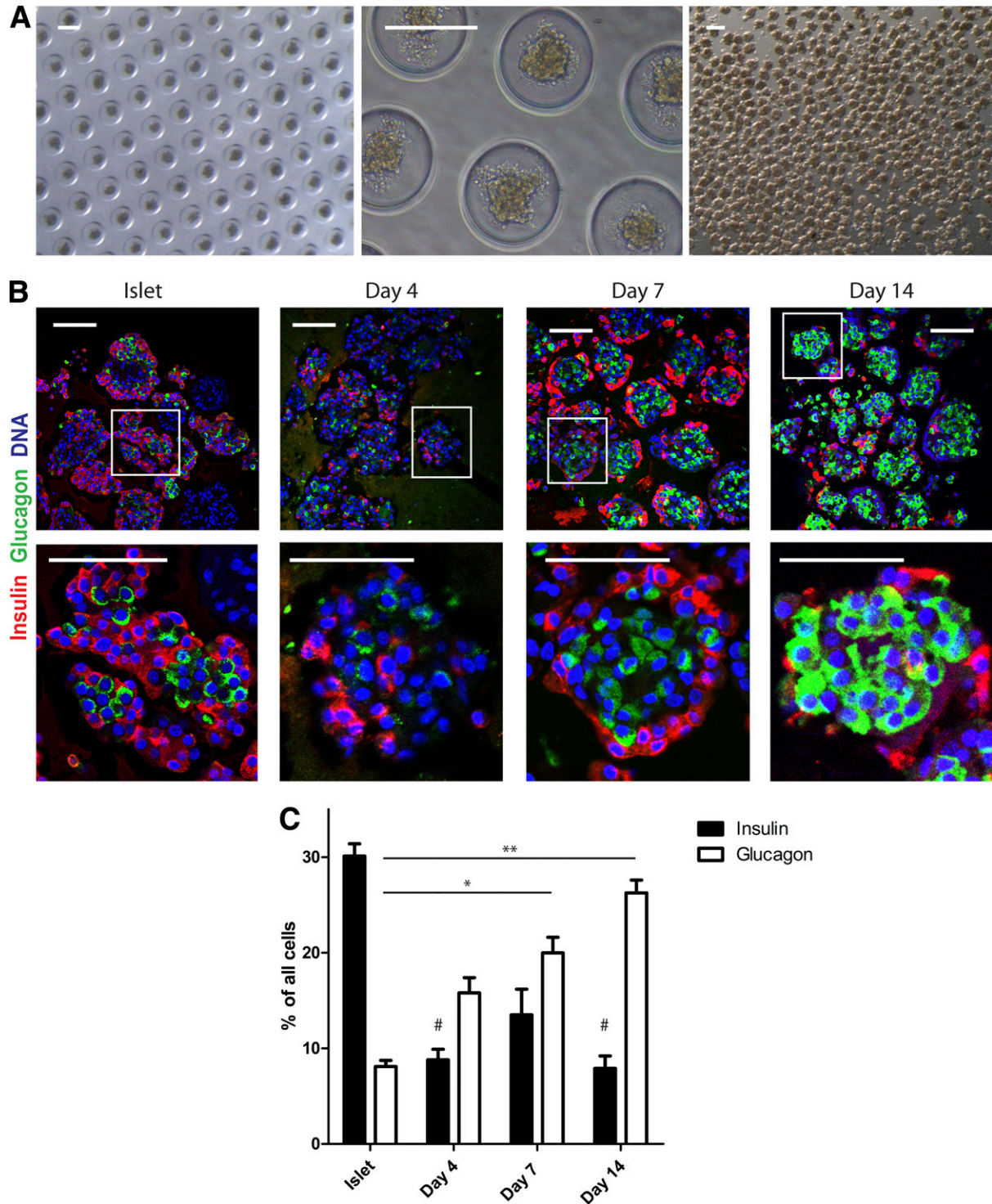


**FIG. 1.** Human islet cell aggregate formation results in an increase in glucagon<sup>+</sup> cells. **A:** Culture of dispersed islet cells in microwells (diameter 200  $\mu$ m) results in homogenously sized islet cell aggregates that remain intact after flushing them out of the microwells. Scale bars: 200  $\mu$ m. **B:** Human islet cell aggregate formation results in a distinct architecture after reaggregation:  $\beta$ -cells (insulin, red) are located at the rim and  $\alpha$ -cells in the center (glucagon, green). Scale bars: 100  $\mu$ m. **C:** Over time, an increased proportion of glucagon<sup>+</sup> cells was present in islet cell aggregates. Data are presented as means  $\pm$  SEM.  $n = 4-9$  donors. \* $P < 0.05$ , \*\* $P < 0.005$  vs. intact islets glucagon; # $P < 0.05$  vs. intact islets insulin.

mmol/L and 20 mmol/L glucose at 37°C. Insulin concentration was determined by ELISA (Mercodia, Uppsala, Sweden).

**Electron microscopy.** Islet cell aggregates were fixed in 1.5% glutaraldehyde and postfixed in 1% osmium tetroxide for conventional transmission electron microscopy. 100-nm-thin sections were poststained with uranyl acetate and lead citrate for ultrastructural analysis. For immunogold labeling, cells were fixed in 0.2% glutaraldehyde and 2% paraformaldehyde. Sections were stained using rabbit anti-GFP (1:100), rabbit anti-glucagon (1:200), and mouse anti-C-peptide (1:1,000; Millipore), and binding was identified using protein A gold (10- or 15-nm labels). Images were made on an FEI Tecnai 12 BioTwin transmission electron microscope. Automated stitching of electron micrographs was performed as previously described (18). Stitched images were quantified using ImageScope software.

**Animal transplantation.** All animal experiments were approved by the Leiden University Medical Center committee for animal ethics. Human islet cell aggregates were transplanted under the kidney capsule of 7- to 12-week-old male NOD/SCID mice. After 2 weeks, grafts were removed for histology.

**Statistical analysis.** Data are expressed as means  $\pm$  SEM unless stated otherwise. Statistical significance of differences between groups were determined by an unpaired Student *t* test or by one-way ANOVA followed by Bonferroni multiple comparisons test, as appropriate. *P* < 0.05 was considered statistically significant.

## RESULTS

**Human islet cell aggregate formation results in an increase in glucagon<sup>+</sup> cells.** Human islets were isolated from pancreas of organ donors (average age 52 years [range 19–71] [Supplementary Table 2]) to  $\geq 70\%$  purity as determined by dithizone staining (Supplementary Fig. 1A). The starting population of intact islets was further characterized by immunostaining and showed  $30.1 \pm 3.9\%$   $\beta$ -cells,  $8.1 \pm 1.9\%$  glucagon-immunoreactive cells, and  $20.6 \pm 5.2\%$  duct cells (Fig. 1 and Supplementary Fig. 1B). For functional and histological studies on islet cell aggregates with a predefined size, human islets were dispersed into single cells followed by reaggregation during culture in agarose-based microwells. One thousand islet cells were seeded per microwell resulting in the formation of human islet cell aggregates with a diameter of  $131 \pm 10 \mu\text{m}$

(Fig. 1A). Compared with intact islets, human islet cell aggregates showed an unusual architecture after 7 days: insulin<sup>+</sup> cells were typically found at the rim, and glucagon<sup>+</sup> cells were located in the center of the aggregates (Fig. 1B). Furthermore, within 4 days of reaggregation the percentage of insulin-immunoreactive cells was significantly decreased (Fig. 1C). This decrease was accompanied by a decrease in gene expression of insulin, *pdx1* and *mafa*. In line, immunolabeling for Pdx1 was decreased after reaggregation (Supplementary Fig. 1C and D). In contrast, the percentage of glucagon-immunoreactive cells was significantly increased during the 14-day reaggregation period, accompanied by a tendency in increased gene expression (Fig. 1C and Supplementary Fig. 1C). We first assessed whether these changes were due to  $\beta$ -cell loss or  $\alpha$ -cell proliferation. TUNEL assay showed overall <2% apoptotic cells, while <1% cell proliferation (Ki67) was observed, of which only 4 of 115 Ki67<sup>+</sup> cells were also glucagon immunoreactive. No significant differences in labeling between isolated islets and at 4, 7, or 14 days of reaggregation were detected that could explain the change in cell composition (Fig. 2).

**Increased number of glucagon<sup>+</sup> cells results from the conversion of  $\beta$ -cells.** In order to explain the decrease in insulin<sup>+</sup> cells and increase in glucagon<sup>+</sup> cells, we hypothesized that a subpopulation of  $\beta$ -cells converts into  $\alpha$ -cells. For tracing  $\beta$ -cell fate directly, dispersed islet cells were transduced with RIP-Cre-ERT2 and CMV-loxP-NEO-STOP-loxP-eGFP lentiviral vectors as shown previously (16,19). Tamoxifen administration results in sustained GFP expression in cells that express insulin at time of the transduction (Fig. 3A and B and Supplementary Fig. 2A, C, and E). We verified the efficiency and specificity of the lineage-tracing system by immunostaining (Supplementary Fig. 2D and E). Importantly, <1% of GFP<sup>+</sup> cells expressed glucagon 1 day after tamoxifen administration (Supplementary Fig. 2E). After 7 days of islet aggregate formation in the

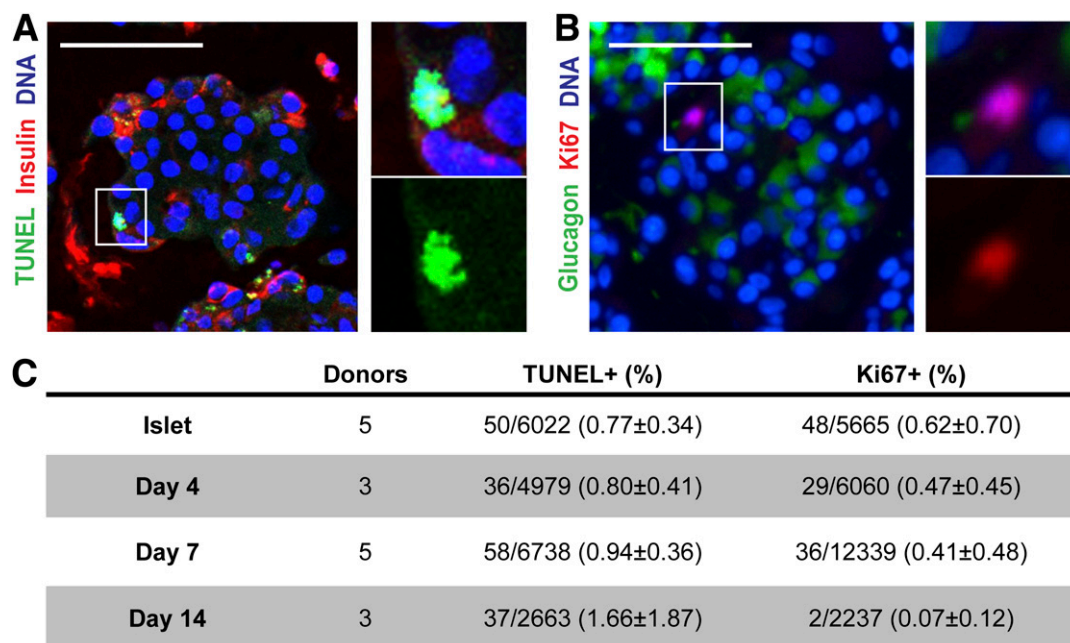


**FIG. 2.** Change in endocrine hormone distribution is not due to apoptosis or proliferation. *A* and *B*: Representative picture of TUNEL assay combined with insulin staining (*A*) and Ki67 staining with glucagon (*B*). *C*: Quantification of apoptotic and proliferating cells defined by the number of positive nuclei in counted cells. Data are presented as means  $\pm$  SEM. *n* = 3–6 donors.

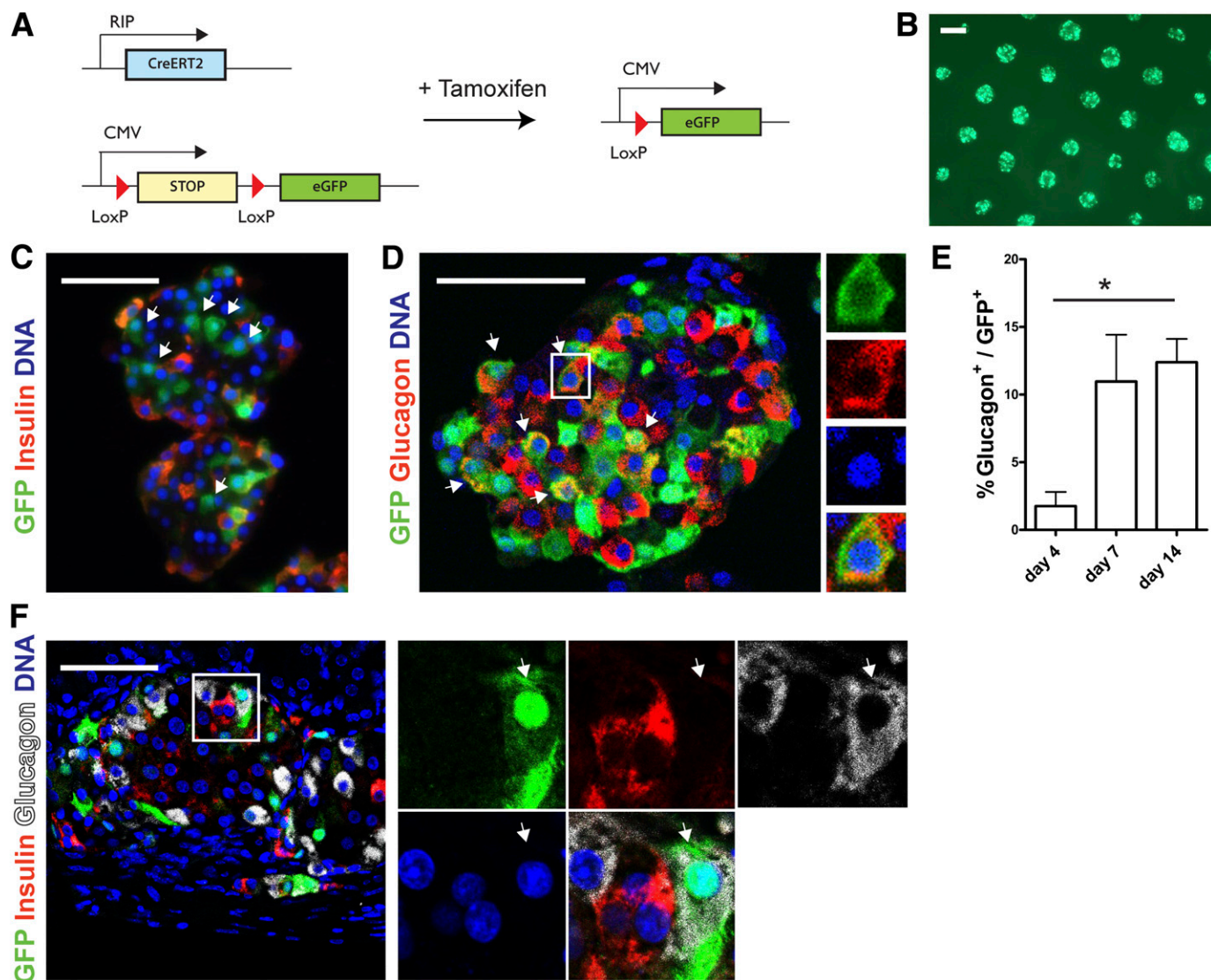


**FIG. 3.** Increased number of glucagon<sup>+</sup> cells results from the conversion of  $\beta$ -cells. **A:** Schematic representation of conditional  $\beta$ -cell-specific lineage tracing using two lentiviral vectors. **B:** Live cell imaging of transduced human islet cell aggregates shows an equal distribution of epifluorescent GFP throughout the microwell chip. **C:** After 7 days of reaggregation, GFP<sup>+</sup> cells are observed that do not express insulin (arrows). **D** and **E:** Glucagon<sup>+</sup>/GFP<sup>+</sup> cells (arrows) are present in human islet cell aggregates (**D**) with increasing numbers over time (**E**). Data are presented as means  $\pm$  SEM.  $n = 3$ –6 donors. \* $P < 0.05$ . **F:** Glucagon<sup>+</sup>/GFP<sup>+</sup> cell (arrows) in a graft after transplantation under the kidney capsule of NOD/SCID mice. Scale bars = 50  $\mu$ m, except for **B:** 200  $\mu$ m.

microwells, not all GFP<sup>+</sup> cells were positive for insulin or C-peptide (Fig. 3C). Intriguingly, up to 15% of GFP<sup>+</sup> cells coexpressed glucagon after 14 days (Fig. 3D and E). This was confirmed by whole mount confocal imaging to detect epifluorescent GFP in cells immunolabeled for glucagon, excluding GFP antibody artifacts (Supplementary Fig. 3A). The presence of GFP<sup>+</sup>/glucagon<sup>+</sup> cells was further confirmed by the detection of glucagon<sup>+</sup> cells after fluorescence-activated cell sorting of the GFP<sup>+</sup> fraction after redispersion of the islet cell aggregates (Supplementary Fig. 3B). GFP<sup>+</sup>/glucagon<sup>+</sup> cells remained present even after transplantation of the islet cell aggregates in vivo under the kidney capsule of NOD/SCID mice (Fig. 3F). The presence of GFP<sup>+</sup> cells did not significantly change over time during the lineage-tracing experiments in vitro and in vivo (data not shown). Of note, both the typical architecture and the cell conversion were observed after reaggregation in six-well ultra-low attachment plates,

excluding the possibility that the microwell culture system is involved directly (data not shown).

**Converted cells have an  $\alpha$ -cell phenotype based on ultrastructural morphology.** For determination of whether the converted  $\beta$ -cells, defined as GFP<sup>+</sup>/glucagon<sup>+</sup> cells, have an  $\alpha$ -cell ultrastructure, electron microscopy was performed. Secretory granules containing insulin can be distinguished from secretory granules containing other islet hormones based on their ultrastructure (20). Immunogold labeling for GFP confirmed colocalization with cells containing insulin granules but also demonstrated colocalization with cells containing more homogeneous, darker, dense granules typical of  $\alpha$ -cells (Fig. 4A and B). Double immunogold labeling for GFP and glucagon showed that 51% of GFP<sup>+</sup> cells contained insulin granules, while 29% contained typical, immunogold-labeled glucagon granules after 14 days (Fig. 4C and Supplementary Fig. 4A and B). Granule morphology and localization were identical

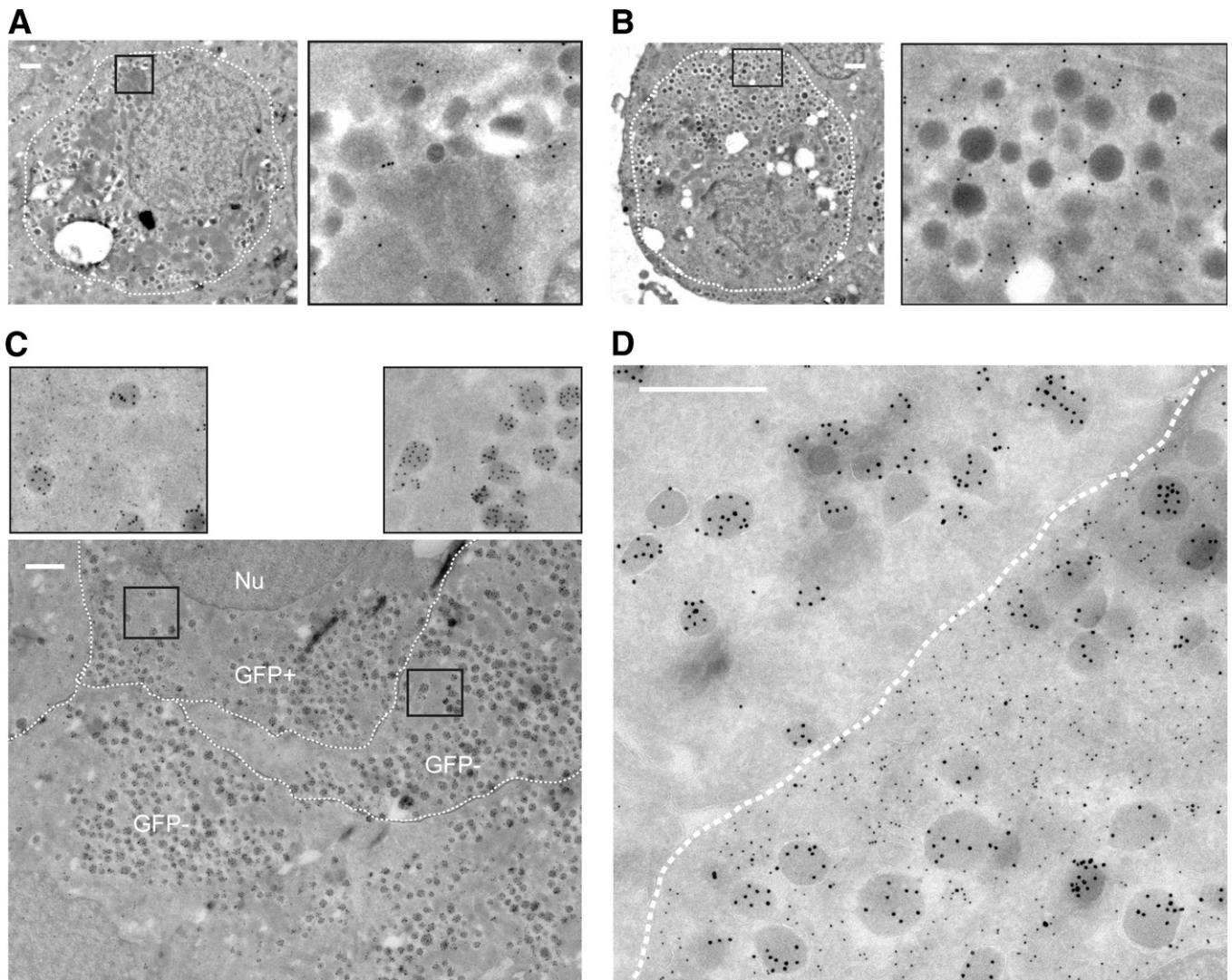


**FIG. 4.** Converted cells are regular  $\alpha$ -cells based on ultrastructural morphology. *A* and *B*: Immunogold labeling for GFP (15-nm gold particles) is present as black dots in both cells with granules with a typical crystalline structure containing insulin (*A*) and cells with more homogenous dark and dense noninsulin granules (*B*). *C* and *D*: Double immunogold labeling for GFP (10-nm gold particles) and glucagon (15-nm gold particles) shows the presence of  $\alpha$ -cell granules in both GFP<sup>+</sup> (converted) and GFP<sup>-</sup> cells (*C*). Immunogold labeling for GFP is absent within granules (*D*). The borders between the cells are marked manually by a broken line (Nu = nucleus). All scale bars = 500 nm.

to those in the GFP-negative  $\alpha$ -cells (Fig. 4C and D). All GFP<sup>+</sup> cells containing the homogeneous, darker, dense granules typical of  $\alpha$ -cells were positive for glucagon immunogold, thereby confirming the preferential conversion of  $\beta$ -cells into  $\alpha$ -cells. Furthermore, of 254 counted cells, 18% of GFP<sup>+</sup> cells were determined as degranulated (<10 granules) and 1 cell contained large amylase granules. Thus, in combination with the lineage tracing, our data demonstrate that mature human  $\beta$ -cells can convert into glucagon-producing  $\alpha$ -cells within days of culture after dispersion and reaggregation.

**$\beta$ -Cell degranulation occurs during human islet cell aggregate formation.** To get an insight into the mechanism of  $\beta$ - to  $\alpha$ -cell conversion, we studied in more detail the early events after dispersion and reaggregation. First of all, using immunostaining no coexpression of glucagon with insulin (Fig. 1B) or C-peptide (data not shown) was detected 4, 7, or 14 days after reaggregation. To ensure the absence of bihormonal cells at the level of single granules, we confirmed these findings by electron microscopy

performing double labelings for glucagon and C-peptide. (Supplementary Fig. 5). However, immunostaining within the first 5 days after reaggregation showed up to 50% of cells negative for insulin but positive for the  $\beta$ -cell-specific transcription factors Pdx1 or Nkx6.1, indicating  $\beta$ -cell degranulation (Fig. 5A and B and data not shown). This was confirmed by ultrastructural analysis showing that 77% of  $\beta$ -cells contained <70 granules after 4 days' reaggregation compared with only 32% of  $\beta$ -cells in intact islets (Fig. 5C and D). Altogether, these data show that dispersion followed by reaggregation results in degranulated  $\beta$ -cells that may still contain specific transcription factors.

**$\beta$ -Cell-to- $\alpha$ -cell transition is demonstrated by glucagon<sup>+</sup> cells that express  $\beta$ -cell transcription factors.** Next we hypothesized that, during the transition phase, cells that lost insulin might coexpress  $\beta$ -cell transcription factors and glucagon. Using  $\beta$ -cell lineage tracing, we show the presence of cells expressing Nkx6.1 or Pdx1 together with glucagon and GFP (Fig. 6A). Interestingly, the percentage of cells coexpressing Pdx1 and glucagon

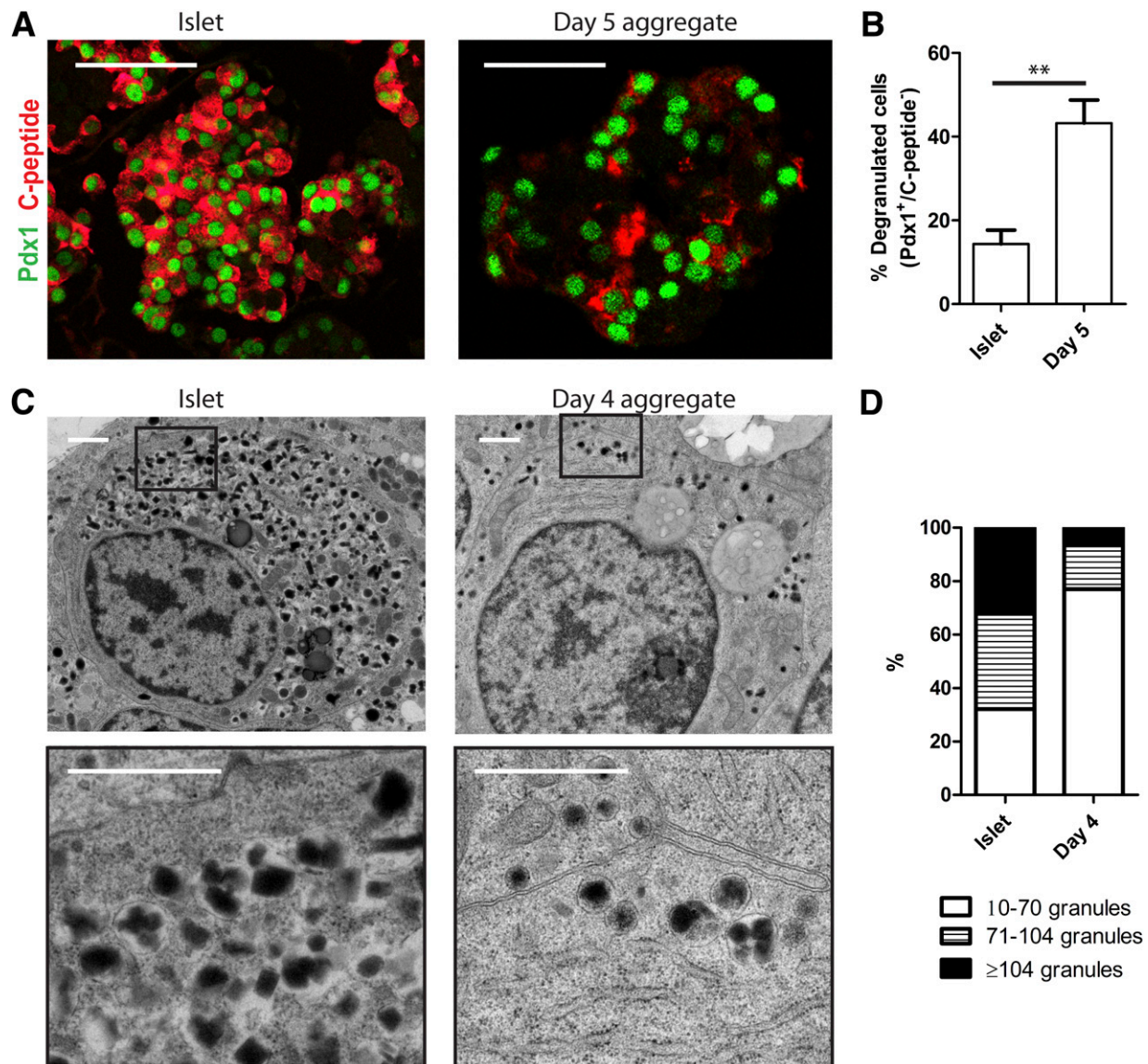


**FIG. 5.** Reaggregation is accompanied by  $\beta$ -cell degranulation. **A:** Immunostaining for Pdx1 (green) and C-peptide (red) in intact islets and 5 days after reaggregation. Scale bars = 100  $\mu$ m. **B:** Quantification of the number of Pdx1<sup>+</sup>/C-peptide<sup>-</sup> cells. Data are presented as means  $\pm$  SEM.  $n = 3$  donors. \*\* $P < 0.005$ . **C:** Electron microscopy photographs showing insulin granules in intact islet  $\beta$ -cells and 4 days after reaggregation. Scale bars = 1  $\mu$ m. **D:** Distribution of the amount of insulin granules per  $\beta$ -cell in intact islets and 4 days after reaggregation (for representation of the distribution, granule number in intact islets was divided in tertiles;  $>50$  cells were counted per condition).

was significantly increased, with almost 3% of glucagon<sup>+</sup> cells at 7 days of reaggregation (Fig. 6B). In addition, using immunoelectron microscopy we observed the presence of GFP<sup>+</sup> cells that contain only very few (<10) glucagon-labeled granules, suggesting recent transition after degranulation (Fig. 6C).

**Arx knockdown inhibits the conversion of  $\beta$ -cells into  $\alpha$ -cells.** *Arx* gene expression was increased in human islet cell aggregates (Fig. 7A). To investigate the role of Arx in the conversion process, we knocked down Arx gene expression using a lentivirus-mediated shRNA against *arx* (shArx). Knockdown was accompanied by a significant decrease in glucagon mRNA and a trend toward induction of *pax4* and insulin gene expression (Fig. 7B).  $\beta$ -Cell-specific lineage tracing revealed that Arx knockdown increased the number of GFP<sup>+</sup>/insulin<sup>+</sup> cells almost twofold, while the number of GFP<sup>+</sup>/glucagon<sup>+</sup> cells decreased by 40% (Fig. 7C–E). Finally, shArx-treated cells showed

higher glucose-induced insulin secretion than cells treated and transduced with a nontarget (control) shRNA (average stimulation index  $5.5 \pm 2.5$  for shCtrl [control] vs.  $8.3 \pm 0.6$  for shArx) in two independent experiments (Fig. 7F). These data demonstrate that the conversion of human  $\beta$ -cells into glucagon-producing  $\alpha$ -cells can be modulated by changing the expression of a key transcription factor.

## DISCUSSION

Mature human  $\beta$ -cells are typically considered as terminally differentiated cells that do not switch their hormone production once fully differentiated. Our results show that human  $\beta$ -cells can convert rapidly and preferentially into glucagon-producing  $\alpha$ -cells without forced expression of exogenous transcription factors. Of importance, the conversion occurred in islets from pancreas of organ donors from different backgrounds, independent of donor factors such as age or sex.

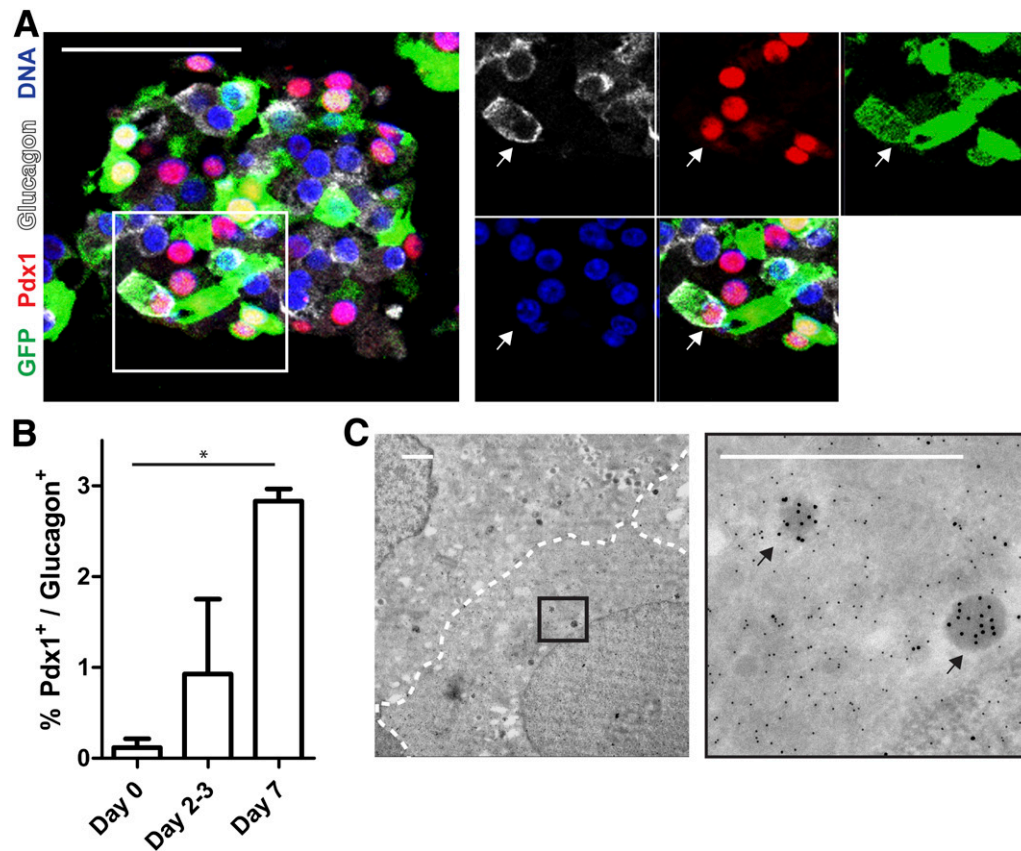


**FIG. 6.**  $\beta$ - to  $\alpha$ -cell transition is marked by the presence of glucagon<sup>+</sup> cells containing  $\beta$ -cell transcription factors. **A:** Immunostaining for GFP (green), Pdx1 (red), and glucagon (white) (arrows in enlargement show triple-positive cell). Scale bar = 100  $\mu$ m. **B:** Quantification of Pdx1<sup>+</sup>/glucagon<sup>+</sup> cells shows an increase during reaggregation ( $n = 3$  donors,  $*P < 0.05$ ). **C:** Double immunogold labeling for GFP (10-nm gold particles) and glucagon (15-nm gold particles) after reaggregation (arrows show single glucagon granules). Scale bar = 1  $\mu$ m.

To date, only a few examples of human cell transdifferentiation have been reported. This usually requires the forced expression of transcription factors or miRNAs to convert human fibroblasts into neurons, hematopoietic progenitors, or brown fat cells (21) or human liver cells into  $\beta$ -cells (22). In our three-dimensional culture system, the dispersion into single cells followed by reaggregation into islet cell aggregates is likely to be a critical step for cell conversion. Previous lineage-tracing studies in human  $\beta$ -cells after dispersion and two-dimensional culture show rapid epithelial-to-mesenchymal transition and no generation of  $\alpha$ -cells (16,23). In this context, the specific architecture of islet cell aggregates is of interest, as  $\beta$ -cells were mainly located at the periphery and  $\alpha$ -cells in the center of the aggregates. Hence, cell-cell and cell-matrix interactions that are disrupted and reestablished, or the changed cell composition and paracrine signaling between islet cells within the aggregates, could be mechanistically linked to our observations.

The mechanisms by which islet cell conversion occur include direct conversion from one endocrine cell type into another or dedifferentiation into a progenitor stage followed by the acquisition of a new endocrine cell phenotype (24). Although the short time period for the conversion to occur and the presence of cells coexpressing glucagon and  $\beta$ -cell-specific transcription factors indicate a direct  $\beta$ - to  $\alpha$ -cell conversion, we cannot rule out a very transient dedifferentiation stage. Along this line, Talchai et al. (25) reported that murine FoxO1-deficient  $\beta$ -cells

first dedifferentiate to a progenitor-like stage expressing Ngn3, Oct4, Nanog, and *L-myc* and subsequently convert into  $\alpha$ -cells. In contrast, Thorel et al. (13) showed direct conversion of  $\alpha$ -cells into  $\beta$ -cells after near-total  $\beta$ -cell ablation through the presence of bihormonal cells (glucagon<sup>+</sup>/insulin<sup>+</sup>), thereby indicating that distinct mechanisms of islet cell conversion may underlie these studies.

Maintenance of  $\beta$ -cell functional maturity is ascribed to two possible mechanisms: either passive or active control (7). Whereas the first option consists of transient activation of transcription factors that lock the cell in a mature state, the second theory relies on continuously active regulators that maintain a differentiated state. We now show that adult human  $\beta$ -cells display potential plasticity, favoring the second hypothesis. Accordingly, this plasticity is accompanied by the downregulation of key  $\beta$ -cell transcription factors such as Pdx1, Nkx6.1, and MafA. Moreover, knockdown of the  $\alpha$ -cell factor Arx could block the conversion, indicating that  $\beta$ -cell plasticity depends on the presence or absence of active modulators. This is in line with recent data from transgenic mouse models (DNMT<sup>-/-</sup> and Nkx2.2<sup>TNmut/TNmut</sup>) that indicate that  $\beta$ -cell identity is maintained by active repression of *Arx* gene transcription (26,27). We extend these observations by showing that Arx is pivotal in the maintenance of a  $\beta$ -cell phenotype in human cells as well, since the downregulation of Arx efficiently blocks the conversion of human adult  $\beta$ -cells.

The (patho)physiological relevance of our findings in humans is unclear. An increased  $\alpha$ -cell mass has been



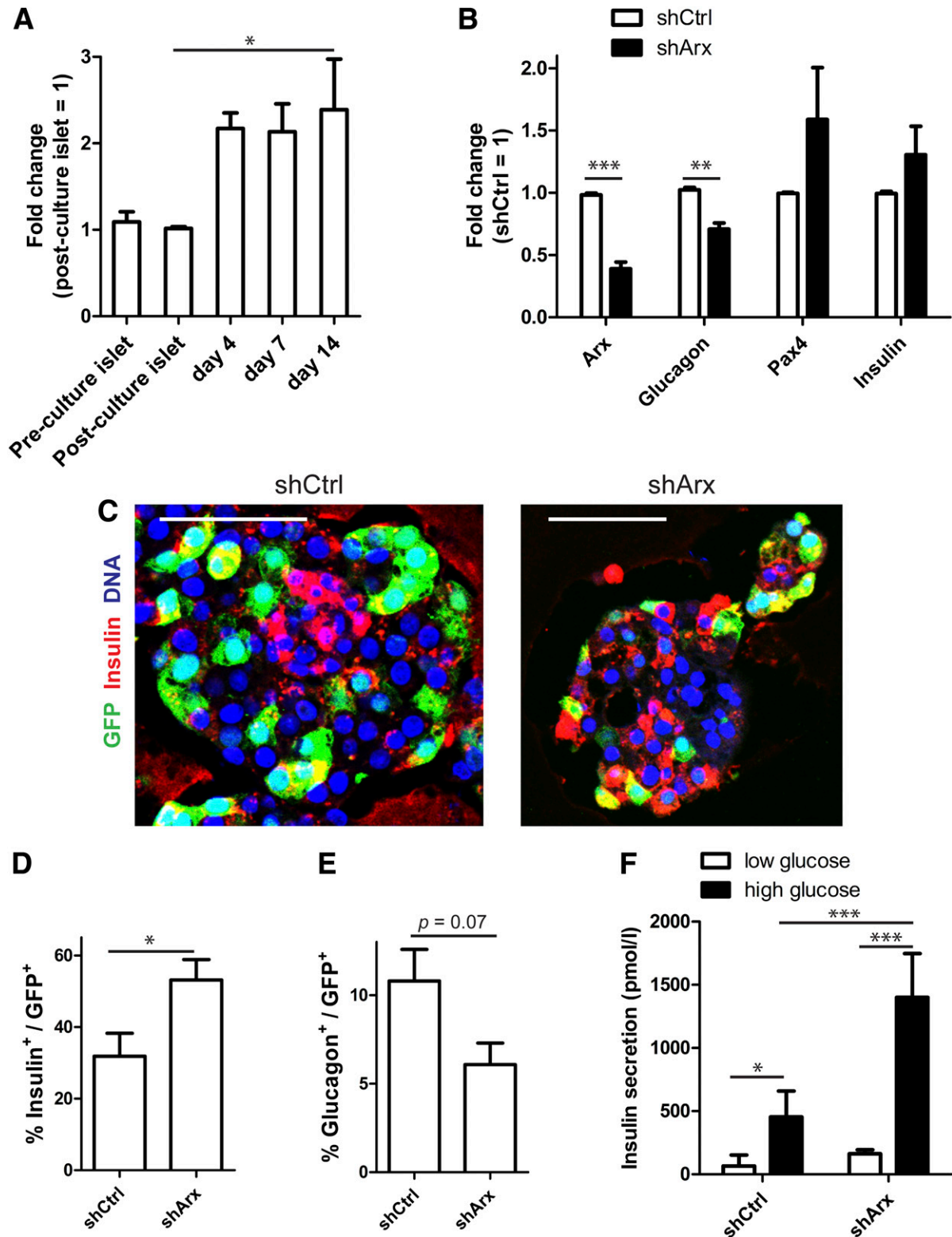


**FIG. 7.** Arx knockdown inhibits the conversion of  $\beta$ -cells into  $\alpha$ -cells. **A:** Arx gene expression in human islet cell aggregates compared with control intact islets ( $n = 3-6$  donors). **B:** shRNA directed against Arx (shArx) results in knockdown of Arx mRNA that is accompanied by changes in glucagon, Pax4, and insulin mRNA levels ( $n = 4$  donors). **C:** Combining  $\beta$ -cell lineage tracing and shRNA treatment shows a large proportion of GFP<sup>+</sup>/insulin<sup>-</sup> cells in shCtrl-treated islet cell aggregates but an increase in GFP<sup>+</sup>/insulin<sup>+</sup> cells in shArx-treated islet cell aggregates. **D** and **E:** The number of remaining  $\beta$ -cells is increased in shArx-treated aggregates compared with shCtrl (**D**), while the number of converted cells is decreased as represented by GFP<sup>+</sup>/glucagon<sup>+</sup> cells (**E**) ( $n = 4$  donors). **F:** Representative graph of a glucose-stimulated insulin secretion assay that shows increased insulin secretion after treatment with shArx (mean  $\pm$  SD of quadruplicates). All experiments were performed after 7–14 days' re-aggregation. Scale bars = 50  $\mu$ m. \* $P < 0.05$ , \*\* $P < 0.005$ , \*\*\* $P < 0.0001$ .

reported in patients with type 2 diabetes (28), a condition that is also characterized by hyperglucagonemia, but this hypothesis has been challenged by a recent study in 50 patients (29). Interestingly, recent work from Talchai et al. (25) associates metabolic stress and type 2 diabetes in mice with  $\beta$ -cell dedifferentiation and conversion into  $\alpha$ -cells (25). This is in line with studies on rats that suffer from chronic hyperglycemia after partial pancreatectomy, showing progressive loss of  $\beta$ -cell differentiation and a strong reduction in expression of  $\beta$ -cell transcription factors (30). In our human model, the substantial  $\beta$ -cell stress that is induced during the dispersion and reaggregation is likely to be an important factor as well. This could explain why near-total  $\alpha$ -cell ablation in mice does not induce conversion of  $\beta$ -cells into  $\alpha$ -cells. Since glucose homeostasis was hardly affected, it may be that  $\beta$ -cell stress in this experiment was limited (31).

Our data have potential relevance for regenerative strategies in diabetes. We show that without genetic modification, conversion of one human islet cell type into another can be achieved. Identification of the signals that are relevant for maintenance and change of islet cell identity could be useful in the quest for generation of  $\beta$ -cells from alternative cell sources.

In conclusion, we provide a proof of principle that postnatal human  $\beta$ -cells can undergo a change in endocrine cell identity. It remains to be investigated whether other human endocrine cell types display the same plasticity and whether this phenomenon plays a role in vivo. Understanding the mechanisms by which adult  $\beta$ -cells maintain or change their identity can have important implications for understanding islet development, (patho)physiology, and regenerative strategies in diabetes.

#### ACKNOWLEDGMENTS

This project is supported by the Dutch Diabetes Research Foundation. Additional funding for our laboratory was obtained from the Diabetes Cell Therapy Initiative, the DON foundation, and the Bontius Foundation.

No potential conflicts of interest relevant to this article were reported.

H.S.S. wrote the manuscript, performed the key experiments, and analyzed data. R.B.G.R. designed and performed stitching of electron microscopy photographs. A.M.M.-K. advised on the electron microscopy. A.A.v.A. provided molds and materials to produce the microwell culture system. M.A.E. provided human islet preparations. A.Z. developed and provided lentivirus productions and gave support in transduction experiments. S.B.-W. advised on the electron microscopy, gave conceptual advice, and helped write the manuscript. T.J.R. gave conceptual advice and helped write the manuscript. R.C.H. developed and provided lentivirus productions and gave support in transduction experiments. H.C. and C.L.M. gave conceptual advice and helped write the manuscript. F.C. and E.J.P.d.K. wrote the manuscript and designed the study. F.C. and E.J.P.d.K. are the guarantors of this work and, as such, had full access to all the data in the study and take responsibility for the integrity of the data and the accuracy of the data analysis.

Parts of this study were presented in abstract form at the 72nd Scientific Sessions of the American Diabetes Association, Philadelphia, Pennsylvania, 8–12 June 2012.

The authors thank J. Onderwater, A. Töns, M. Rabelink, and S. Cramer for expert technical help (Leiden University Medical Center). The authors thank S. Efrat (Tel Aviv University) and P. Ravassard (Université Pierre et Marie Curie, Paris, France) for kindly providing lineage tracing lentiviral constructs.

#### REFERENCES

- Cabrera O, Berman DM, Kenyon NS, Ricordi C, Berggren PO, Caicedo A. The unique cytoarchitecture of human pancreatic islets has implications for islet cell function. *Proc Natl Acad Sci USA* 2006;103:2334–2339
- Brissova M, Fowler MJ, Nicholson WE, et al. Assessment of human pancreatic islet architecture and composition by laser scanning confocal microscopy. *J Histochem Cytochem* 2005;53:1087–1097
- Bosco D, Armanet M, Morel P, et al. Unique arrangement of alpha- and beta-cells in human islets of Langerhans. *Diabetes* 2010;59:1202–1210
- Seymour PA, Sander M. Historical perspective: beginnings of the beta-cell: current perspectives in beta-cell development. *Diabetes* 2011;60:364–376
- Courtney M, Pfeifer A, Al-Hasani K, et al. In vivo conversion of adult  $\alpha$ -cells into  $\beta$ -like cells: a new research avenue in the context of type 1 diabetes. *Diabetes Obes Metab* 2011;13(Suppl. 1):47–52
- Sander M, Sussel L, Connors J, et al. Homeobox gene *Nkx6.1* lies downstream of *Nkx2.2* in the major pathway of beta-cell formation in the pancreas. *Development* 2000;127:5533–5540
- Szabat M, Lynn FC, Hoffman BG, Kieffer TJ, Allan DW, Johnson JD. Maintenance of  $\beta$ -cell maturity and plasticity in the adult pancreas: developmental biology concepts in adult physiology. *Diabetes* 2012;61:1365–1371
- Ferber S, Halkin A, Cohen H, et al. Pancreatic and duodenal homeobox gene 1 induces expression of insulin genes in liver and ameliorates streptozotocin-induced hyperglycemia. *Nat Med* 2000;6:568–572
- Kojima H, Fujimiya M, Matsumura K, et al. NeuroD-beta-cellulin gene therapy induces islet neogenesis in the liver and reverses diabetes in mice. *Nat Med* 2003;9:596–603
- Collombat P, Xu X, Ravassard P, et al. The ectopic expression of Pax4 in the mouse pancreas converts progenitor cells into alpha and subsequently beta cells. *Cell* 2009;138:449–462
- Zhou Q, Brown J, Kanarek A, Rajagopal J, Melton DA. In vivo reprogramming of adult pancreatic exocrine cells to beta-cells. *Nature* 2008;455:627–632
- Yang YP, Thorel F, Boyer DF, Herrera PL, Wright CV. Context-specific  $\alpha$ -to- $\beta$ -cell reprogramming by forced Pdx1 expression. *Genes Dev* 2011;25:1680–1685
- Thorel F, Népoté V, Avril I, et al. Conversion of adult pancreatic alpha-cells to beta-cells after extreme beta-cell loss. *Nature* 2010;464:1149–1154
- Ricordi C, Lacy PE, Finke EH, Olack BJ, Scharp DW. Automated method for isolation of human pancreatic islets. *Diabetes* 1988;37:413–420
- Rivron NC, Rouwkema J, Truckenmüller R, Karperien M, De Boer J, Van Blitterswijk CA. Tissue assembly and organization: developmental mechanisms in microfabricated tissues. *Biomaterials* 2009;30:4851–4858
- Russ HA, Ravassard P, Kerr-Conte J, Pattou F, Efrat S. Epithelial-mesenchymal transition in cells expanded in vitro from lineage-traced adult human pancreatic beta cells. *PLoS ONE* 2009;4:e6417
- Carlotti F, Bazuine M, Kekarainen T, et al. Lentiviral vectors efficiently transduce quiescent mature 3T3-L1 adipocytes. *Mol Ther* 2004;9:209–217
- Faas FG, Avramut MC, van den Berg BM, Mommaas AM, Koster AJ, Ravelli RB. Virtual nanoscopy: generation of ultra-large high resolution electron microscopy maps. *J Cell Biol* 2012;198:457–469
- Bar-Nur O, Russ HA, Efrat S, Benvenisty N. Epigenetic memory and preferential lineage-specific differentiation in induced pluripotent stem cells derived from human pancreatic islet beta cells. *Cell Stem Cell* 2011;9:17–23
- Pisania A, Weir GC, O'Neil JJ, et al. Quantitative analysis of cell composition and purity of human pancreatic islet preparations. *Lab Invest* 2010;90:1661–1675
- Vierbuchen T, Wernig M. Direct lineage conversions: unnatural but useful? *Nat Biotechnol* 2011;29:892–907
- Sapir T, Shternhall K, Meivar-Levy I, et al. Cell-replacement therapy for diabetes: Generating functional insulin-producing tissue from adult human liver cells. *Proc Natl Acad Sci USA* 2005;102:7964–7969
- Russ HA, Bar Y, Ravassard P, Efrat S. In vitro proliferation of cells derived from adult human beta-cells revealed by cell-lineage tracing. *Diabetes* 2008;57:1575–1583

24. Zhou Q, Melton DA. Extreme makeover: converting one cell into another. *Cell Stem Cell* 2008;3:382–388
25. Talchai C, Xuan S, Lin HV, Sussel L, Accili D. Pancreatic  $\beta$  cell dedifferentiation as a mechanism of diabetic  $\beta$  cell failure. *Cell* 2012;150:1223–1234
26. Papizan JB, Singer RA, Tschen SI, et al. Nkx2.2 repressor complex regulates islet  $\beta$ -cell specification and prevents  $\beta$ -to- $\alpha$ -cell reprogramming. *Genes Dev* 2011;25:2291–2305
27. Dhawan S, Georgia S, Tschen SI, Fan G, Bhushan A. Pancreatic  $\beta$  cell identity is maintained by DNA methylation-mediated repression of Arx. *Dev Cell* 2011;20:419–429
28. Deng S, Vatamaniuk M, Huang X, et al. Structural and functional abnormalities in the islets isolated from type 2 diabetic subjects. *Diabetes* 2004;53:624–632
29. Henquin JC, Rahier J. Pancreatic alpha cell mass in European subjects with type 2 diabetes. *Diabetologia* 2011;54:1720–1725
30. Jonas JC, Sharma A, Hasenkamp W, et al. Chronic hyperglycemia triggers loss of pancreatic beta cell differentiation in an animal model of diabetes. *J Biol Chem* 1999;274:14112–14121
31. Thorel F, Damond N, Chera S, et al. Normal glucagon signaling and  $\beta$ -cell function after near-total  $\alpha$ -cell ablation in adult mice. *Diabetes* 2011;60:2872–2882